Pergamon

SCIENCE DIRECT®

Tetrahedron 59 (2003) 3581–3592

TETRAHEDRON

A DFT study on the 1,3-dipolar cycloaddition reactions of *C*-(methoxycarbonyl)-*N*-methyl nitrone with methyl acrylate and vinyl acetate

Pedro Merino,[a,*] Julia Revuelta,[a] Tomas Tejero,[a] Ugo Chiacchio,[b] Antonio Rescifina[b,*] and Giovanni Romeo[c]

[a]*Departamento de Quimica Organica, Facultad de Ciencias, ICMA, Universidad de Zaragoza-CSIC, Zaragoza E-50009, Spain*
[b]*Dipartimento di Scienze Chimiche, Università di Catania, Viale Andrea Doria 6, Catania 95125, Italy*
[c]*Dipartimento Farmaco-Chimico, Università di Messina, Viale SS. Annunziata, Messina 98168, Italy*

Received 16 January 2003; revised 13 March 2003; accepted 2 April 2003

Abstract—In the 1,3-dipolar cycloaddition of glyoxylic nitrones with electron-poor and electron-rich alkenes, the configurational instability of the nitrone leads to parallel models when regio- and stereoselectivities are rationalized. The energetics of the cycloaddition reactions have been investigated through molecular orbital calculations at the B3LYP/6-31-G(d) theory level. By studying different reaction channels and reagent conformations, leading to a total of sixteen transition structures for each dipolarophile, the regio- and stereochemical preferences of the reaction are discussed.

1. Introduction

The synthetic utility of 1,3-dipolar cycloadditions (1,3-DC) between nitrones and alkenes has been thoroughly established.[1] The importance of these reactions stems from the utility of the obtained isoxazolidines as synthetic intermediates.[2]

According to the MO perturbation treatment reported by Huisgen,[3] nitrones are dipoles of type II, i.e. the energetic splitting between HOMO and LUMO orbitals of dipole and dipolarophile are similar. As a consequence, both electron-donating and -attracting substituents in 1,3-dipole and dipolarophile accelerate the reaction, and thus normal ($HOMO_{dipole}$-controlled) and inverse ($LUMO_{dipole}$-controlled) demand reactions can take place.

Several computational studies have been carried out to understand the origins of the regio- and stereoselectivities of the reaction,[4] and from these studies density functional theory (DFT) has emerged as a very convenient approach for obtaining reliable results at a low computational cost. In this context, a rationale to account for the reactivity and selectivity of electron-rich dipolarophiles, including Lewis acid and solvent effects, has been reported by Domingo.[5] The reaction of heterocyclic nitrones with electron-deficient dipolarophiles has been previously studied by one of us,[6] and Tanaka and Kanemasa have evaluated the effect of Lewis acids with the same type of dipolarophiles.[7] DFT calculations have also been used for evaluating the influence of inherent electronic effects and solvent polarity in the regioselectivity of 1,3-dipolar cycloadditions.[8]

The synthetic utility of glyoxylic acid derived nitrones **1** has been widely demonstrated in one of our laboratories[9] and by other groups.[10] Despite this synthetic activity no theoretical studies with nitrones **1** have been reported. It is known that nitrones having an electron-withdrawing group at the α position, like **1**, are configurationally unstable and they can be found as a mixture of *E*/*Z* isomers[11] (Scheme 1). The equilibrium between these isomers has been studied in solution and a dependence on the polarity of the solvent has been found.[12] The *E*/*Z* isomerization of nitrones has invoked to occur via ring opening of oxaziridines.[13] The presence of Lewis acids can also induce such an isomerization.[14]

As a consequence of the interconversion between *E*/*Z* isomers, parallel models are always proposed for cycloaddition reactions of **1**. In all cases it is possible to explain

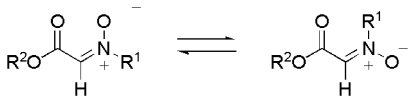

Scheme 1.

Keywords: methyl acrylate; vinyl acetate; glyoxylic nitrones.
* Corresponding authors. Tel./fax: +34-976-762075;
e-mail: pmerino@posta.unizar.es; arescifina@dipchi.unict.it

0040–4020/03/$ - see front matter
doi:10.1016/S0040-4020(03)00547-7

the obtention of the *trans* isomer by invoking either an *endo* approach to the *Z*-isomer or an *exo* approach to the *E*-isomer. Similarly, the obtention of *cis* isomers can be explained through an *exo* approach to the *Z*-isomer or an *endo* approach to the *E*-isomer (Scheme 2). Moreover, in addition to the 3,5-regiosiomers, illustrated in Scheme 2, 3,4-regioisomers might also be obtained. So, a total of eight different approaches should be considered.

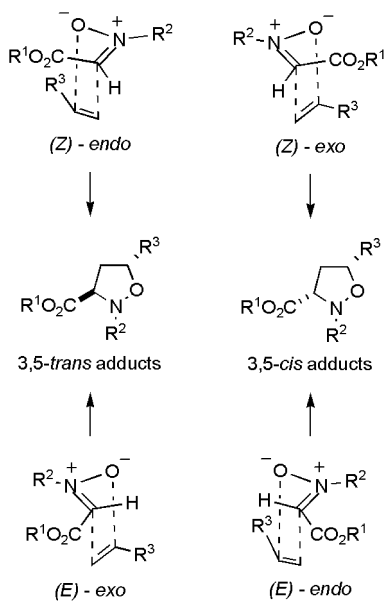

Scheme 2.

The reaction of nitrones **1** with electron-deficient alkenes usually give *trans* adducts preferentially.[15] It has been invoked that these reactions take place through an *E-exo* approach due to the higher stability of the *E*-isomer.[16] However, it is also possible to propose that the reaction undergoes through an *endo* approach (preferred in all cycloaddition reactions with electron-deficient alkenes) to the more reactive *Z*-isomer.[17] The corresponding parallel can be done with electron-rich alkenes, too. Despite this controversy there is no theoretical studies concerning cycloadditions of nitrones bearing electron-withdrawing groups that clearly discriminate between the possible approaches.

With the aim of defining the preferred approaches for cycloaddition reactions of nitrones **1** and to introduce additional details in the commonly accepted general model of 1,3-DC of nitrones, we report herein a systematic theoretical investigation of 1,3-dipolar cycloadditions of **1** (R_1=R_2=Me) using DFT calculations on all possible [3+2] cycloaddition pathways. Electron tuning of the reactivity was studied for methyl acrylate and vinyl acetate.

2. Computational methods

DFT calculations were carried out with the G98 system of programs.[18] Critical points (reactants, transition structures and products) were fully characterized as minima or first-order saddle points by diagonalizing the Hessian matrices of the optimized structures at the B3LYP/6-31G* level.[19] All the critical points were further characterized by analytic computation of harmonic frequencies at the B3LYP/6-31G* level. Transition structures were found to have only one negative eigenvalue with the corresponding eigenvector involving the formation of the newly created C–C and C–O bonds. Vibrational frequencies were calculated (1 atm, 298.15 K) for all B3LYP/6-31G* optimized structures and used, unscaled, to compute both ZPVE and activation energies. The electronic structures of critical points were studied by the natural bond orbital (NBO) method.[20] The enthalpy and entropy changes were calculated from standard statistical thermodynamic formulas.[21] The intrinsic reaction coordinates[22] (IRC analysis) were also calculated to analyze the mechanism in detail for all the transition structures obtained.

We studied regio- and diastereoselectivity for the reaction of (*E*)- and (*Z*)-**1** with methyl acrylate **2** and vinyl acetate **3**. For each transition state the most stable conformations of methyl acrylate[23] and vinyl acetate[24] have been chosen. On the other hand, both *s-cis* and *s-trans* conformations of (*E*)- and (*Z*)-**1** have been evaluated. Figure 1 displays the conformational features of the reaction partners.

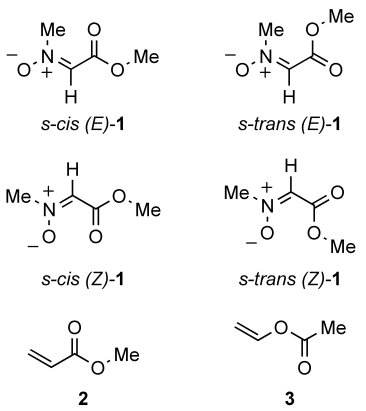

Figure 1. Reactants.

We have considered two reaction channels, *ortho* and *meta*, corresponding to the formation of 3,5 and 3,4-disubstituted isoxazolidines, respectively. *endo* and *exo* approaches to *E*- and *Z*- isomers completed the study. Consequently, 16 transition states leading to four cycloadducts have been located for each dipolarophile. The nomenclature used for defining stationary points is given in Scheme 3.

3. Results and discussion

3.1. Reactants

The lowest energy structure of nitrones **1** corresponds to the *s-cis E* isomer. The *s-trans* conformation is higher in energy by 3.00 kcal/mol in terms of free energy (Table 1). Nitrone *Z* is also higher in energy than nitrone *E* by more than 3.70 kcal/mol. For (*Z*)-**1**, however, the *s-cis* and *s-trans* conformations are very nearly equal in energy (within 0.07 kcal/mol at the B3LYP/6-31G(d) level).

The same order of stability emerged by the total delocalization energies (Table 1) calculated using a

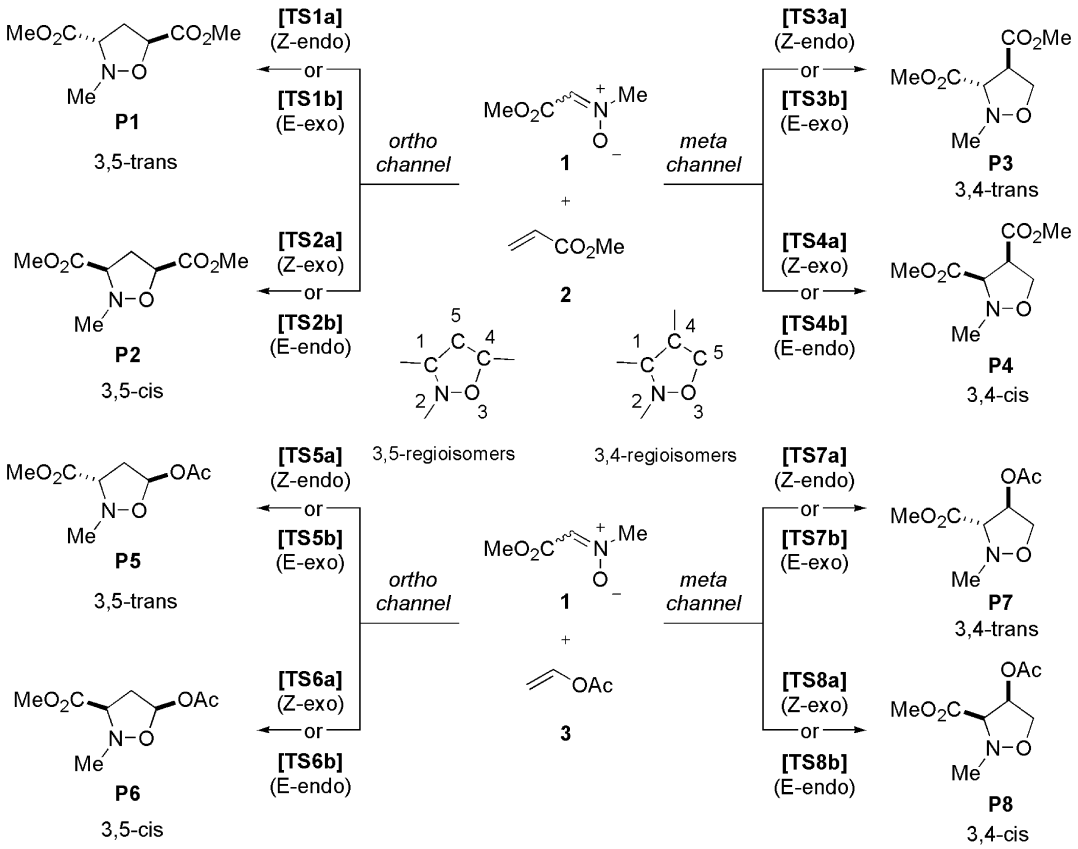

Scheme 3.

secondary-order perturbation theory (SOPT) analysis of the Fock matrix in NBO Basis according to the definition of delocalization energy given by Weinhold.[25] In particular the *s-cis* (*E*)-**1** conformer is more stable than *s-trans* (*E*)-**1** because of the two principal stabilizing delocalization energies $\pi\ C_1-N_2\rightarrow\pi^*\ C_5-O_6$ (13.66 kcal/mol) and $nO_6\rightarrow\sigma^*C_{4-H_{12}}$ found in the former. These values are higher than those found for the *s-trans* conformer ($\pi\ C_1-N_2\rightarrow\pi^*\ C_5-O_6$ (12.46 kcal/mol) and $nO_7\rightarrow\sigma^*\ C_4-H_{12}$ (4.46 kcal/mol)) by 1.20 and 1.37 kcal/mol, respectively. The $n\rightarrow\sigma^*$ interactions were also confirmed by the Mulliken population analysis (MPA), which gives a qualitative indicator for the amount of electron density shared by two atoms. We have found O_6H_{12} positive overlap density values (0.032 and 0.022 for the *s-cis* and *s-trans* (*E*)-**1** conformers, respectively) in agreement with the preferred *s-cis* stability. On the other hand, in the two (*Z*)-**1** conformers there no interaction between O_6 carboxylic oxygen and the H_{12} hydrogen. Moreover, the O_3O_6 and the O_3O_7 overlap densities, corresponding to the *s-cis* and *s-trans* conformers, respectively, have a negative value of −0.001 thus indicating a lone-pair/lone-pair repulsion. These two factors destabilize the (*Z*)-isomer over the (*E*) one.

All conformers studied are planar (Fig. 2). The lower energy conformer for each isomer corresponds to that having the larger ∠N−C−C angle. Thus, these angles in *s-cis* (*E*)-**1** and *s-trans* (*Z*)-**1** (131.8° and 127.5°) are larger than in *s-trans* (*E*)-**1** and *s-cis* (*Z*)-**1** (126.6° and 123.3°), respectively. For (*E*)-**1** the lower energy *s-cis* conformer corresponds to that having the smaller dipole moment (2.21 D). The largest dipole moment corresponds to *s-cis* (*Z*)-**1** (4.53 D) in which the carbonyl group and the nitrone oxygen are oriented in a parallel way.

3.2. Prediction of regiochemistry

A simple way to foresee the regiochemistry of the 1,3-DC reactions consists of using the charges obtained from

Table 1. B3LYP/6-31G(d) free energies (*G*) (hartrees) relative free energies (Δ*G*) (kcal/mol), electronic energies (*E*) (hartrees) and relative electronic energies (Δ*E*) (kcal/mol) together with the delocalization energies (kcal/mol) for reactants

	E	Δ*E*	*G*	Δ*G*	Delocalization energy[a]	Dipole moment
s-cis (*E*)-**1**	−436.867216	0.00	−436.909646	0.00	524.43	2.21
s-trans (*E*)-**1**	−436.861322	4.06	−436.904864	3.00	509.11	4.14
s-cis (*Z*)-**1**	−436.860751	3.97	−436.903599	3.79	507.58	4.53
s-trans (*Z*)-**1**	−436.860888	3.70	−436.903.709	3.73	513.13	2.36
2	−306.365295	–	−306.402235	–	332.90	1.50
3	−306.369179	–	−306.407043	–	295.55	1.73

[a] Calculated according to the definition of delocalization energy given in Ref. 25.

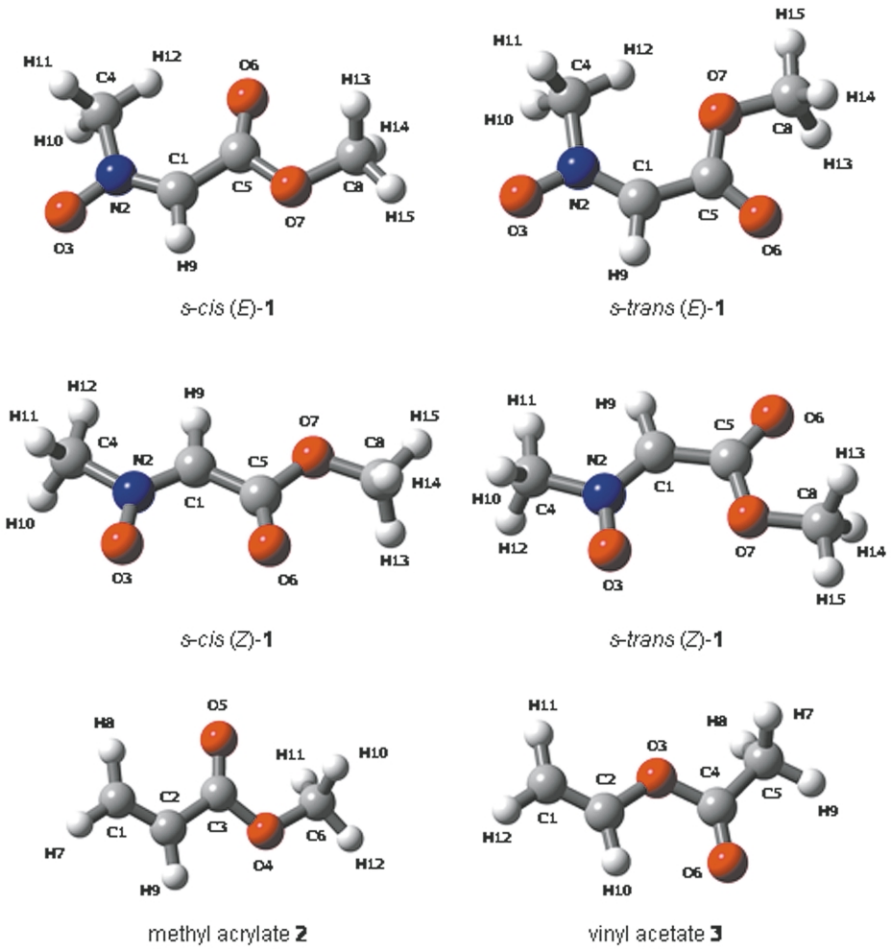

Figure 2. B3LYP/6-31G(d) optimized structures of the reactants.

Natural Population Analysis,[26] that show less basis set dependence with respect to Mulliken charges and are better descriptors of the molecular density distribution.[27] In the case at hand nitrones **1** have, on average, a negative charge on both C_1 (−0.15) and O_3 (−0.44) atoms, so as compound **2** on C_1 (−0.337) and C_2 (−0.344) atoms, whereas vinyl acetate **3** has a negative charge on C_1 (−0.49) and a positive one on C_2 (+0.10). In the reaction of **1** with **2** the more nucleophilic oxygen of nitrone can equally attach the C_1 and C_2 atom of methyl acrylate, because the very small difference in the charges between these two atoms (Δq=0.007), leading to an almost equimolar mixture of 4- and 5-substituted regioisomers. On the other hand, in the reaction of **1** with **3**, the major isomer formed (the 5-substituted) is the isomer with the oxygen of nitrone (the most negative end of dipole) attached to the positive C_2 of vinyl acetate and the C_1 of nitrone attached to C_1 of **3** (that is the most negative respect to the carbon atom of nitrone).

We have also analyzed the cycloaddition reactions using the global and local indexes (defined in the context of the DFT[28]), which are useful tools to understand the reactivity of molecules in their ground states. The electronic chemical potential μ is usually associated with the charge transfer ability of the system in its ground state geometry and it can be approximated, using Koopmans' theorem, to the half value of the sum of the one-electron energies of the frontier molecular orbitals (FMO) HOMO and LUMO.[28a,29] The chemical hardness η is considered to be a measure of the stability of a system: the system having the maximum hardness being the most stable.[30] Essentially the hardness is approximated to be the difference of LUMO and HOMO energy. The chemical softness parameter S is strictly related to the chemical hardness and it is due to the inverse of 2η.[28]

Besides these indexes it is also possible to define the global electrophilicity power ω which measures the stabilization in energy when the system acquires an additional electronic charge ΔN from the environment. The approximate expression for ω, in the ground-state parabola model, is[31]

$$\omega = \frac{\mu^2}{2\eta} \tag{1}$$

and it may be classified within a unique relative scale in order to evaluate the polarity of transition state structures. Both Diels-Alder reactions[32] and 1,3-dipolar cycloadditions[33] can be evaluated using such an absolute scale. The values of these parameters for compounds **1**, **2** and **3**, calculated with the reported formulas, are listed in Table 2.

The electronic chemical potential of methyl acrylate **2** is similar to that of nitrone **1**, thereby indicating that there is only a slight charge transfer between the two reactants. Instead, the chemical potential of vinyl acetate **3** is lower

Table 2. Global properties (electronic chemical potential μ, chemical hardness η and chemical softness S values are in a.u.; electrophilicity power ω values are in eV) and local softness (s^+ for nucleophilic and s^- for electrophilic attack) of nitrone **1**, methyl acrylate **2** and vinyl acetate **3**

		μ	η	S	ω	s^-		s^+		s^-		s^+	
						C_1	O_3	C_1	O_3	C_1	C_2	C_1	C_2
(*E*)-**1**	*s-cis*	−0.15785	0.16982	2.94	2.00	0.952	1.046	0.447	0.570				
	s-trans	−0.15709	0.16848	2.97	1.99	0.941	1.078	0.448	0.579				
(*Z*)-**1**	*s-cis*	−0.15340	0.17707	2.82	1.81	0.403	0.998	0.471	0.510				
	s-trans	−0.15369	0.17635	2.83	1.82	0.922	1.016	0.461	0.526				
2		−0.15841	0.22875	2.18	1.49					0.129	−0.072	0.599	0.255
3		−0.12992	0.20545	2.43	1.12					0.836	0.403	0.515	0.189

than the chemical potential of nitrone **1** so indicating that a net charge transfer will take place from **3** to **1**. Indeed, the electrophilicity differences between *s-cis* (*E*)-**1** and **2** ($\Delta\omega$=0.51 eV) indicates a lower polar character for this cycloaddition than for the reaction between **1** and **3** ($\Delta\omega$=0.88 eV). Both $\Delta\omega$ values are characteristic of non-polar (pericyclic) reactions[32,33] as it is also indicated by the low charge transfer found in all cases. Whereas the global parameters help understanding the behavior of the system, in a more local approach, the same parameters, also emerge as a useful tool for rationalizing, interpreting and predicting diverse aspects of chemical bonding and reaction mechanism. Recently, local softness *s* has been applied successfully for explaining the regiochemistry in more complex pericyclic reactions.[34] However, in order to explain the regiochemistry of a multicenter reaction the HSAB principle needs to be considered in a local sense in addition to local softness. Chandra and Nguyen have correlated the idea of the local HSAB concept and regioselectivity defining a quantity that suggests a measure of predominance of one reaction over the other.[34b,35] This quantity, said 'delta' (Δ) is so defined:

$$\Delta_{ij}^{kl} = (s_i - s_k)^2 + (s_j - s_l)^2 \quad (2)$$

where *i* and *j* are the atoms of a molecule **A** involved in the formation of a cycloadduct with atoms *k* and *l* of a molecule **B**, and s_is are the appropriate type of atomic softness (if s_i and s_j are electrophilic then s_k and s_l are obviously nucleophilic). According to Eq. (2) the reaction associated with a lower Δ value will be the preferred one.

The local softness *s* was calculated as a product *fS*, where *f* is the condensed form of Fukui functions calculated as reported elsewhere,[36] utilizing the NBO derived charges. The values obtained for s_is and the corresponding Δs values, referred at both *meta* and *ortho* channels, for the cycloadditions of **1** with **2** and **3** are reported in Tables 2 and 3 respectively.

In the case of the 1,3-DC of **1** with **2**, or with the nitrone as nucleophile or as electrophile the Δ values for both *meta* and *ortho* channels are similar. Although the *ortho* channel predominates in both cases, it is expected the formation of both regioisomers. For the reaction between **1** and **3**, we should consider only the Δ values for a $LUMO_1$–$HOMO_3$ approach, in accord to global parameter analysis. The *ortho* regioisomer is clearly predominant and almost exclusively formed, in contrast with the experience. So, although the regioselectivity of a pericyclic process characterized by a low charge transfer is mainly controlled by the FMO interactions, in this case, surprisingly, the simplest analysis based upon charges of the atoms directly involved in the formation of the two new sigma bond is clever to predict the experimental results very well.

Table 3. Reverse energy gaps (eV) between molecular orbitals for the reaction of **1** with **2** and **3**

s-cis (*E*)-**1**+**2**				*s-cis* (*E*)-**1**+**3**			
$HOMO_1$–$LUMO_2$		$LUMO_1$–$HOMO_2$		$HOMO_1$–$LUMO_3$		$LUMO_1$–$HOMO_3$	
Δ_{meta}	Δ_{ortho}	Δ_{meta}	Δ_{ortho}	Δ_{meta}	Δ_{ortho}	Δ_{meta}	Δ_{ortho}
0.75	0.68	0.51	0.46	0.92	0.86	0.18	0.07

3.3. Cycloadditions with methyl acrylate

3.3.1. Energies of the transition structures. The absolute and relative free and electronic energies with respect to reactants for the 16 transition structures located for the reaction between **1** and **2** are collected in Table 4.

The predicted activation free energies for the *ortho* channel are, in general terms, lower than those corresponding to the

Table 4. B3LYP/6-31G(d) relative free energies (ΔG) (kcal/mol) and relative electronic energies (ΔE) (kcal/mol) for the reaction of nitrones **1** with methyl acrylate **2**

		Direct ΔE^a	Inverse ΔE^b	Direct ΔG^a	Inverse ΔG^b
TS1a	*s-cis*	11.94	31.93	24.75	31.51
	s-trans	12.11	32.11	24.85	31.61
TS1b	*s-cis*	12.90	27.82	25.51	27.20
	s-trans	16.01	30.93	28.35	30.04
TS2a	*s-cis*	13.44	33.17	26.63	32.94
	s-trans	12.98	32.71	26.27	32.59
TS2b	*s-cis*	12.88	26.43	25.57	27.17
	s-trans	15.13	28.68	27.73	29.34
TS3a	*s-cis*	11.77	31.38	24.88	31.47
	s-trans	12.17	31.78	25.34	31.93
TS3b	*s-cis*	13.50	28.07	26.37	27.98
	s-trans	18.10	32.67	29.00	30.61
TS4a	*s-cis*	14.61	32.42	28.10	31.98
	s-trans	13.69	31.50	27.51	31.39
TS4b	*s-cis*	12.74	26.43	26.07	26.11
	s-trans	15.38	29.08	28.43	28.46
P1		−20.08		−6.83	
P2		−19.81		−6.39	
P3		−19.70		−6.66	
P4		−17.90		−3.95	

[a] Referred to *s-cis* (*E*)-**1**+**2** (see Table 1 for values) for reactions with *E* isomer and to *s-trans*(*Z*)-**1**+**2** (see Table 1 for values) for reactions with *Z* isomer.
[b] Referred to the corresponding products.

meta channel. Accordingly, it can be predicted that the 3,5-regioisomers will be formed preferentially, in agreement with the experimental observations. When couples of transition structures leading to the same compound are compared in terms of *endo*/*exo* and *Z*/*E* preferences, it can be seen that the activation barriers for the *Z*-*endo* approach are lower than those for *E*-*exo* approaches, namely *s-cis* **TS1a**<*s-cis* **TS1b**, *s-trans* **TS1a**<*s-trans* **TS1b**, *s-cis* **TS3a**<*s-cis* **TS3b** and *s-trans* **TS3a**<*s-trans* **TS3b**. There is, however, a very small difference of only 0.1 kcal/mol between the three transition structures lower in energy, *s-cis* **TS1a**, *s-trans* **TS1a** and *s-cis* **TS3a**. Although these values indicate a predominant *endo* approach for the reaction, it is not possible to elucidate which is the preferred conformation of the nitrone in the transition state. Looking strictly at the absolute energy values, only in the case of a *Z*-*exo* approach (**TS2a** and **TS4a**) the *s-trans* conformation is preferred to the *s-cis* conformation in the transition state. In cases in which the preferences for a *Z* isomer and an *endo* approach are competitive (**TS2a** vs **TS2b** and **TS4a** vs **TS4b**) there is no marked difference in the energy barriers, thus indicating opposite effects between the more reactive *Z* isomer and the preferred *endo* attack.

In all transition structures in which the *E* isomer is implied, those corresponding to *s-cis* conformations of the nitrone are shorter in energy than those related with *s-trans* conformations. On the other hand, in the case of *Z* isomers nearly equal values of energy are observed for *s-cis* and *s-trans* conformations in some cases, not being possible to clearly define a preferred conformation. This trend is parallel to that found for the ground states in which whereas no energetic differences were observed between *s-cis* and *s-trans* (*Z*)-**1**, a higher stability was observed for *s-cis* (*E*)-**1**.

For the reaction with methyl acrylate, it is predicted a slight preference for an *endo* approach (characteristic of electron-poor alkenes like **2**) and it can be inferred a higher reactivity of the *Z* isomer.

For **TS1a**, **TS2b**, and **TS3a**, **TS4b**, which corresponds to the transition structures for the *endo* approach in the *meta* and *ortho* channels, respectively, MPA provides some evidence for secondary orbital interaction (SOI) between the two reactants.[37] In fact the **TS1a** shows a positive overlap density of 0.015, 0.005 and 0.005 for O_3H_{21}, C_4O_7 and $O_{13}H_{20}$ respectively; similar interaction can be seen in **TS2b** (C_4O_7=0.002 and O_3H_{22}=0.010), **TS3a** (O_4C_{21}=0.016 and $C_{11}H_{17}$=0.003) and **TS4b** (O_4H_{23}=0.014 and O_5C_{11}=0.007). On the other hand, these interactions are not observed for the *exo* approach with the exception of **TS1b**, where are less intense (O_3H_{21}=0.011, C_4O_7=0.002, $O_{13}H_{19}$=0.003). Moreover, if we take in account that these 1,3-DC are mainly conducted in THF or toluene at reflux temperatures, i.e. at 70–110 °C, on the basis of the reverse barrier energies reported in Table 4, we can assume that the reactions at hand are reversible and then under thermodynamic control, so that the **P4** product, possessing a ΔG of −3.95 kcal/mol, under these conditions is not obtained. These data are in good agreement with the observed stability and the experimental results observed in 1,3-DC for similar compounds.[38]

3.3.2. Geometries of the transition structures. The optimized geometries of eight transition structures corresponding to the reaction of **E** and **Z** isomers, and leading to the four possible products **P1**,**P2**,**P3**, and **P4**, are illustrated in Figure 3. Only the more stable *s-cis* or *s-trans* conformers are shown (the rest of geometries are available from the authors).

For the lower energy *meta* transition structures, the lengths of the C–C forming bonds (2.03–2.09 Å) are markedly shorter than the lengths of the C–O ones (2.20–2.25 Å). As expected for electron-deficient dipolarophiles, the situation is reversed for the *ortho* channel, the length of the C–C forming bonds (2.27–2.36 Å) being clearly larger than those of the C–O forming bonds (1.87–1.92 Å). Taking into consideration that C–O sigma bonds are shorter than C–C sigma bonds, the difference of the lengths of the two forming bonds are inside of the range of a concerted process but with a significant asynchronicity. It is well known that when a 1,3-DC cycloaddition presents asynchronous TSs, diradical structures could in principle be involved.[39] This as been ruled out repeating the TSs calculations using the Keywords STABLE, present in Gaussian 98, at both RB3LYP/6-31G* and UB3LYP/6-31G* levels. In all the cases the wavefunction resulted stable under the perturbations considered.

A remarkable difference between transition structures concerns the conformation of the forming isoxazolidine ring, defined by C_1–N_2–O_3–C_4–C_5 and C_1–N_2–O_3–C_5–C_4 atoms for *meta* and *ortho* channels, respectively. Transition structures of (*E*)-**1** show positive values, in the range of 51.6° to 59.2°, of $\angle O_3$–N_2–C_1–$C_5(C_4)$ dihedral angle, the larger values corresponding to the *meta* channel. These transition states (**TS1b**, **TS2b**, **TS3b**, **TS4b**) also presented positive, but smaller, values (2.1° to 10.8°) for the $\angle O_3$–C_4–C_5–C_1 (or $\angle O_3$–C_5–C_4–C_1) dihedral angle. For transition structures corresponding to (*Z*)-**1** negative values are observed for both dihedral angles. The larger values correspond to $\angle O_3$–N_2–C_1–$C_5(C_4)$ angle (−24.6° to −58.1°) and the smaller values to $\angle O_3$–$C_4(C_5)$–$C_5(C_4)$–C_1 angle (0.0° to −9.7°). Noteworthy, transition structures corresponding to a 3,4-*endo* attack present four atoms in a plane, the only out-of-plane atom being the nitrogen one.

3.3.3. Bond order and charge analysis. The concept of bond order (BO) can be utilized to obtain a more deepen analysis of the extent of bond formation or bond breaking along a reaction pathway. This theoretical tool has been used to study the molecular mechanism of chemical reactions. To follow the nature of the formation process for C_1–C_5 (C_1–C_4) and C_4–O_3 (C_5–O_3) bonds, the Wiberg bond indexes[40] have been computed by using the NBO population analysis as implemented in Gaussian 98. The results are included in Table 5.

The general analysis of the bond order values for all the TSs structures showed that the cycloaddition process is asynchronous with an interval of 0.286–0.471 and 0.299–0.484 for the *meta* and *ortho* channels, respectively. Moreover, for the *meta* channel the BOs for the forming C_1–C_5 bonds are in the range of 0.431–0.471 and have greater values than that for the forming C_4–O_3 bonds that are in the range of

Table 5. Delocalization energies (ΔE in kcal/mol) from reactants to TSs, bond orders (Wiberg indexes) for the two forming bonds in the TSs and charge transfer (a.u.) in terms of the residual charge of the nitrone fragment in the transition state

		ΔE^a	C_1-C_5[b], C_1-C_4[c]	C_4-O_3[b], C_5-O_3[c]	NPA q_{CT} (e)
TS1a	*s-cis*	108.44	0.442	0.294	0.049
	s-trans	72.73	0.441	0.291	0.047
TS1b	*s-cis*	242.31	0.466	0.304	0.034
	s-trans	121.27	0.456	0.300	0.030
TS2a	*s-cis*	79.88	0.431	0.286	0.041
	s-trans	72.73	0.431	0.289	0.036
TS2b	*s-cis*	224.10	0.471	0.301	0.049
	s-trans	259.19	0.464	0.296	0.048
TS3a	*s-cis*	71.94	0.299	0.484	0.034
	s-trans	81.57	0.302	0.477	0.035
TS3b	*s-cis*	177.99	0.314	0.468	0.030
	s-trans	230.32	0.315	0.456	0.024
TS4a	*s-cis*	112.37	0.300	0.452	0.035
	s-trans	116.47	0.304	0.455	0.026
TS4b	*s-cis*	263.64	0.327	0.479	0.029
	s-trans	180.86	0.319	0.479	0.037

[a] Calculated using a secondary-order perturbation theory (SOPT) analysis of the Fock matrix.
[b] Referred to 3,5-regioisomers.
[c] Referred to 3,4-regioisomers.

0.286–0.304. Instead, for the *ortho* channel the BOs corresponding to the forming C_1-C_4 bonds (0.299–0.327) have a lower values than that for the former C_5-O_3 (0.452–0.484). These data show a change of asynchronicity on the bond formation process for the two regioisomeric pathways although the extent of asynchronicity is the same for the two channels.

The natural population analysis[41] allows to evaluate the charge transferred between the two reactants at the TSs geometry. The charge transfer in terms of the residual charge on the nitrone, for all the optimized TSs, is shown in Table 5. Although the positive values are indicative of an electron flow from the HOMO of nitrone to the LUMO of the methyl acrylate, their magnitudes revealing an almost neutral reaction. Indeed, since both reagents have quite similar electronic chemical potential values, it could be expected that no charge transfer between the reagents takes place.

There is an important increasing of the delocalization energy from reactants to TSs as inferred from the SOPT analysis shown in Table 5. Even though it cannot be assumed a complete correlation between the energies of the TSs and the total energies of delocalization, an examination of the contribution due to the inter-reactants delocalizations, accounts for the SOI pointed out by the MPA. Thus, the **TS1a** is particularly stabilized by a $n\rightarrow\pi^*$ (2.40 kcal/mol) delocalization of the oxygen long pairs of the nitrone moiety with the antibonding orbital of the carboxylic double bond of the olefin moiety. Moreover, there are two neat stabilization due to a $n\rightarrow\sigma^*$ (1.43 kcal/mol) of the long pair on the carboxylic oxygen of **2** with the C–H single bond of the methyl substituent present on **1**, and a $\pi\rightarrow\sigma^*$ (0.65 kcal/mol) of the carboxylic double bond ever with the same C–H single bond. On the other hand, for **TS1b** only a $n\rightarrow\pi^*$ (1.16 kcal/mol) stabilization $O_{nitrone}-C{=}O_{dipolarophile}$ is found. These data are in an excellent agreement with the major stability of **TS1a** vs **TS1b** due to the strongest SOI achieved in the *endo* approach. The same analysis extended to all TSs lead to parallel conclusions.

Table 6. B3LYP/6-31G(d) relative free energies (ΔG) (kcal/mol) and relative electronic energies (ΔE) (kcal/mol) for the reaction of nitrones **1** with vinyl acetate **3**

		Direct ΔE^a	Inverse ΔE^b	Direct ΔG^a	Inverse ΔG^b
TS5a	*s-cis*	16.94	44.60	29.90	44.12
	s-trans	16.79	44.46	29.66	43.88
TS5b	*s-cis*	15.31	37.54	28.07	36.96
	s-trans	17.97	38.24	30.49	36.37
TS6a	*s-cis*	14.93	41.93	28.28	42.14
	s-trans	15.38	43.04	28.44	42.66
TS6b	*s-cis*	16.89	37.16	29.62	35.50
	s-trans	19.49	42.52	32.23	42.37
TS7a	*s-cis*	18.14	39.62	30.93	39.07
	s-trans	19.01	45.22	31.31	43.92
TS7b	*s-cis*	18.15	34.58	31.50	34.37
	s-trans	21.11	35.22	34.35	34.92
TS8a	*s-cis*	19.71	40.07	33.02	38.78
	s-trans	18.33	39.81	32.15	40.28
TS8b	*s-cis*	16.82	30.93	31.17	31.74
	s-trans	21.05	37.44	34.98	37.02
P5		−27.75		−14.29	
P6		−27.08		−13.93	
P7		−21.57		−8.21	
P8		−20.45		−5.84	

[a] Referred to *s-cis* (*E*)-**1**+**3** (see Table 1 for values) for reactions with *E* isomer and to *s-trans* (*Z*)-**1**+**3** (see Table 1 for values) for reactions with *Z* isomer.
[b] Referred to the corresponding products.

3.4. Cycloadditions with vinyl acetate

3.4.1. Energies of the transition structures. The absolute and relative free energies for the sixteen transition structures located for the reaction between **1** and **3** are indicated in Table 6.

As in the case of methyl acrylate the activation free energies for the *ortho* channel (3,5-regioisomers) are lower in energy than those corresponding to the *meta* channel (3,4-regiosiomers). Also in this case it is possible to predict the predominant formation of 3,5-regioisomers in good agreement with experimental observations.[38h,38i,42] The two transition structures lower in energy are *s-cis* **TS-5b** and *s-cis* **TS6a** corresponding to *exo* approaches of the dipolarophile to *E* and *Z* isomers, respectively. These data agree with an expected *exo* preference for a relatively electron-rich alkene like **3**. The difference of only 0.2 kcal/mol between *s-cis* **TS-5b** and *s-cis* **TS6a** indicates that a mixture of products **P5** and **P6** will be obtained, although such a small difference does not allow to evaluate the results quantitatively. A preference for *s-cis* conformations is observed in the transition structures, particularly for (*E*)-**1**. For **TS5a** and **TS8a**, corresponding to 3,5-*endo* and 3,4-*exo* approaches, the *s-trans* conformation is preferred although small differences in energy are obtained.

For the cycloaddition with vinyl acetate it can be predicted an *exo* approach of the dipolarophile. Even preferred *s-cis* conformation of nitrone can be inferred. However, it is difficult to predict what isomer (*E* or *Z*) is the most reactive.

Even in this case, for **TS5b** and **TS6a**, which corresponds to the transition structures for the *exo* approach in the *meta* channel, MPA provides some evidence for their major stability with respect to the corresponding **TS5a** and **TS6b** due to SOI effect. In fact, the **TS5b** shows a positive overlap density of 0.005 for O_4C_6 and a negative ones of −0.017 for O_4H_9; on the contrary, **TS5a** shows a positive overlap density of 0.004 for O_4C_6 and a negative ones of −0.020 for O_4H_9 so accounting for its minor stability. Similar interaction are involved in **TS6a** (O_4C_6=0.005 and O_4O_9=−0.017), and **TS6b** (O_4C_6=0.004 and O_4O_9=−0.021). These interactions are reversed for **TS7a**,**b** and **TS8a**,**b** justifying their preference for the *endo* approach.

Moreover, this reaction, with the exception of **TS8b**, shows higher values for the inverse energy barrier (Table 6) than those corresponding to the reaction between **1** and **2**, and then it should be irreversible at the experimental conditions employed. Nevertheless, in this case the kinetic and thermodynamic products are coincident and then the only formation of **P5** and **P6** is noticeable, in agreement with experimental results reported in literature for analogue reactions.[38]

3.4.2. Geometries of the transition structures. The optimized geometries of eight transition structures corresponding to the reaction of *E* and *Z* isomers, and leading to the four possible products **P5**, **P6**, **P7**, and **P8**, are illustrated in Figure 4. Only the more stable *s-cis* or *s-trans* conformers are shown (the rest of geometries are available from the authors).

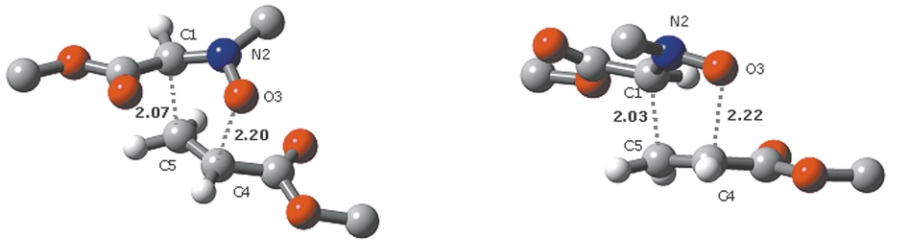

s-cis **TS1a**

s-cis **TS1b**

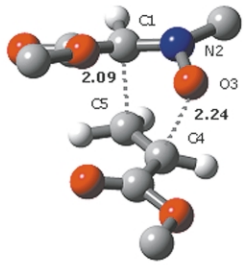

s-trans **TS2a**

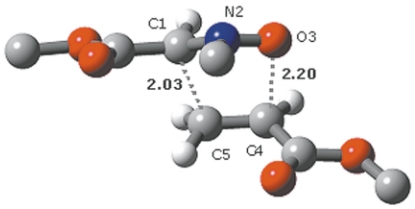

s-cis **TS2b**

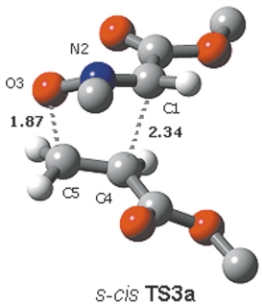

s-cis **TS3a**

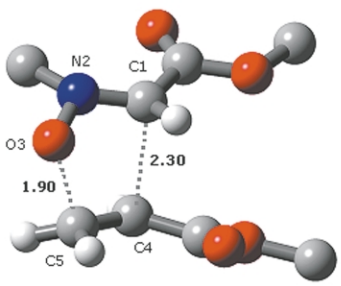

s-cis **TS3b**

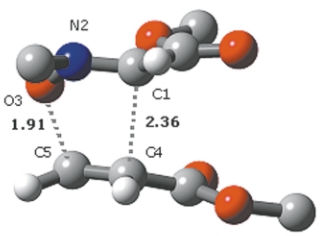

s-trans **TS4a**

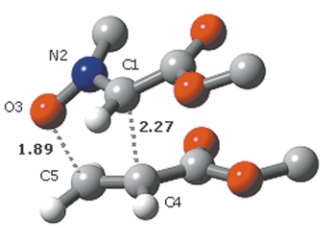

s-cis **TS4b**

Figure 3. Optimized geometries at B3LYP/6-31G(d) level for transition structures leading to **P1**, **P2**, **P3**, and **P4**. Some hydrogen atoms have been omitted for clarity. Distances of forming bonds are given in angstroms.

For cycloaddition of vinyl acetate with (*E*)- and (*Z*)-**1**, the lengths of the forming bonds are closer than for the reaction with methyl acrylate. The lengths of the C–C forming bonds (2.14–2.25 Å) are slightly longer than the C–O forming bonds (2.00–2.13 Å). This rule remains valid for *meta* and *ortho* channels, although in the former, the lengths of both forming bonds are closer than in the latter. Indeed, rather similar forming bonds lengths are found for **TS6a** and **TS5b**. Since C–O bonds are shorter than C–C bonds these data clearly show a concerted process.

The geometrical disposition of the five atoms implied in forming new bonds (C_1, N_2, O_3, C_4 and C_5) follow a similar trend to that of transition structures corresponding to methyl acrylate. However, some deviation of the general trend is found. Thus, transition structures related to *E*-isomer show positive values of $\angle O_3–N_2–C_1–C_5(C_4)$ (51.0°–56.6°) and $\angle O_3–C_4(C_5)–C_5(C_4)–C_1$ (11.0°–13.5°) dihedral angles, with the exception of **TS6b** and **TS7b** which present values of the latter dihedral angle near to zero whatever the conformation (*s-trans* or *s-cis*) is.

In the case of transition structures related with (*Z*)-**1**, negative values (−49.0° to −52.8°) of $\angle O_3–N_2–C_1–C_5(C_4)$ are found. Smaller but still negative values are observed for $\angle O_3–C_5(C_4)–C_4(C_5)–C_1$ (−11.2° to −13.2°). Now the exception comes from **TS5a**, which shows small positive values for $\angle O_3–C_5(C_4)–C_4(C_5)–C_1$ (3.0° and 3.3° for *s-trans* and *s-cis*, respectively), and **TS8a**, which shows almost zero values for the same dihedral angle.

3.4.3. Bond order and charge analysis. The general analysis of the bond order values for all the TSs structures showed that the cycloaddition process is slightly asynchronous with an interval, in the Wiberg bond indexes, of 0.313–0.404 and 0.357–0.414 for the *meta* and *ortho* channels respectively. Moreover, for the *meta* channel the BOs for the forming $C_1–C_5$ bonds are in the range of 0.380†0.404 and have greater values than those observed the forming $C_4–O_3$ bonds, which are in the range of 0.313–0.346. Instead, for the *ortho* channel the BOs corresponding to the forming $C_1–C_4$ bonds (0.357–0.387) have lower values than that of the former $C_5–O_3$ (0.391–0.414). These data show a change of asynchronicity on the bond formation process for the two regioisomeric pathways with the *meta* channel scarcely more asynchronous than the *ortho* one. Furthermore, in the *meta* channel, the more stable **TS5b** and **TS5a** are the most asynchronous. This analysis is in agreement with the corresponding imaginary frequency values that are generally lower for the more asynchronous TSs.[43] How said is valid as well for the comparison of the reactions of the nitrone **1** with compounds **2** and **3**: the more asynchronous TSs correspond the lower imaginary frequency values.

The charge transfer, evaluated by the natural population analysis, in terms of the residual charge on the nitrone, for all the optimized TSs, is shown in Table 7. The negative values are indicative of an electron flow from the HOMO of the vinyl acetate to the LUMO of the nitrone, in agreement to the lower value of the electronic chemical potential of **3** (μ=−0.12992) with respect to that of **1** (μ=−0.15785).

Table 7. Delocalization energies (ΔE in kcal/mol) from reactants to TSs, bond orders (Wiberg indexes) for the two forming bonds in the TSs and charge transfer (a.u.) in terms of the residual charge of the nitrone fragment in the transition state

		ΔE[a]	$C_1–C_5$,[b] $C_1–C_4$[c]	$C_4–O_3$,[b] $C_5–O_3$[c]	NPA q_{CT} (e)
TS5a	*s-cis*	109.04	0.381	0.343	−0.051
	s-trans	112.04	0.380	0.338	−0.051
TS5b	*s-cis*	318.81	0.404	0.331	−0.065
	s-trans	147.54	0.399	0.326	−0.067
TS6a	*s-cis*	379.88	0.387	0.322	−0.071
	s-trans	111.07	0.380	0.313	−0.065
TS6b	*s-cis*	372.50	0.401	0.346	−0.053
	s-trans	249.37	0.397	0.341	−0.055
TS7a	*s-cis*	369.24	0.372	0.395	−0.047
	s-trans	78.56	0.373	0.391	−0.047
TS7b	*s-cis*	−12.91	0.379	0.414	−0.049
	s-trans	−13.82	0.382	0.405	−0.051
TS8a	*s-cis*	133.51	0.361	0.402	−0.045
	s-trans	171.13	0.357	0.408	−0.060
TS8b	*s-cis*	−40.18	0.387	0.408	−0.051
	s-trans	−20.45	0.387	0.399	−0.045

[a] Calculated using a secondary-order perturbation theory (SOPT) analysis of the Fock matrix.
[b] Referred to 3,5-regioisomers.
[c] Referred to 3,4-regioisomers.

From the results of the SOPT analysis showed in Table 7 there is an important increment in the delocalization energy from reactants to TSs, with the exception of **TS7b** and **TS8b** that show negative values. Again, although there is not a complete correlation between the energies of the TSs and the total energies of delocalization, an examination of the contributions due to the inter-reactants delocalizations, accounts for the SOI pointed out by the MPA. Thus, the **TS5b** is stabilized by a $n\rightarrow\sigma^*$ (1.14 kcal/mol) delocalization of the oxygen long pairs of the nitrone moiety with the antibonding orbital of the oxygen single bond of the olefin moiety; the same stabilization, in **TS5a**, is only 0.67 kcal/mol. Similar results were obtained for **TS6a** ($n\rightarrow\sigma^*$; 1.11 kcal/mol) and **TS6b** ($n\rightarrow\sigma^*$; 0.62 kcal/mol). These observations are in agreement with the major stability observed for **TS5b** vs **TS5a** and for **TS6a** vs **TS6b** due to the strongest SOI achieved in the *exo* approach. The same analysis extended to TSs corresponding to *ortho* channel lead to parallel conclusions, but with the inversion of *exo*/*endo* stability.

4. Conclusions

In cycloadditions with methyl acrylate the predicted preference for a *Z-endo* transition structure is substantial. A theoretical preference for 3,5-regioisomers is also observed and the predominance of *trans* adducts are correctly predicted with a difference of more than 1.0 kcal/mol. The theoretical preference for *s-cis* conformations over *s-trans* conformations is less pronounced and in some cases differences of only 0.1 kcal/mol are observed. These low energy differences in predicted barriers for *s-cis* vs *s-trans* are in no way reliable; the differences may not have the accuracy for quantitative predictions, and we believe that these are qualitatively correct and account for the selectivities calculated for the studied reactions. Indeed, such small differences highlights the difficulty of predicting

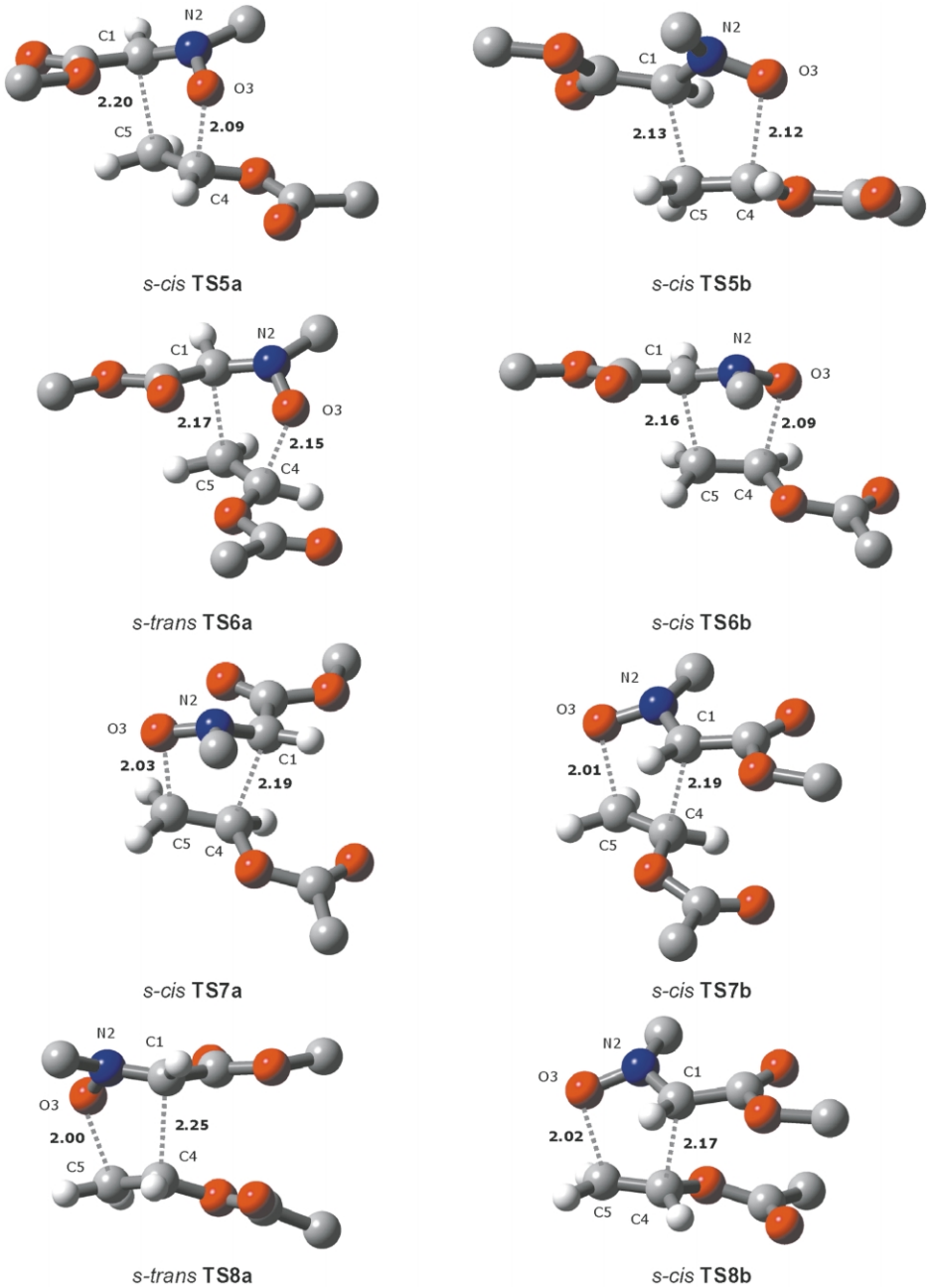

Figure 4. Optimized geometries at B3LYP/6-31G(d) level for transition structures leading to **P5**, **P6**, **P7**, and **P8**. Some hydrogen atoms have been omitted for clarity. Distances for forming bonds are given in angstorms.

the transition structure which operate in the formation of each product. In some instances calculations predict barrier differences of <0.3 kcal/mol. Preferences based on these energy differences are very weak by themselves since the results could be reverted by steric reasons in similar reactions with different groups. The results obtained agree with the experimental findings for both methyl acrylate and vinyl acetate. Consideration of the ground state not always lead to successful rationalization of the selectivity.[44]

Acknowledgements

We thank for their support our programs: the Spanish Ministry of Science and Technology (MCYT) and FEDER Program (Project CASANDRA, BQU2001-2428) and the Government of Aragon (Project P116-2001); the Ministry of Instruction, University and Scientific Research (Rome, Italy) and Italian C. N. R. (Roma). Professor L. R. Domingo (University of Valencia, Spain) is gratefully acknowledged for reading the manuscript and quite helpful discussions.

References

1. (a) Tufariello, J. J. *1,3-Dipolar Cycloaddition Chemistry*; Padwa, A., Ed.; Wiley-Interscience: New York, 1984; Vol. 2. (b) Paquette, L. A. *Comprehensive Organic Synthesis*; Trost,

B. M., Fleming, I., Eds.; Pergamon: Oxford, 1991; Vol. 5. Chapter 3.
2. (a) Frederickson, M. *Tetrahedron* **1997**, *53*, 403–425. (b) Gothelf, K. V.; Joörgensen, K. A. *Chem. Rev.* **1998**, *98*, 863–909. (c) Gothelf, K. V.; Joörgensen, K. A. *Chem. Commun.* **2000**, 1449–1458.
3. (a) Huisgen, R. *Advances in Cycloaddition*; Curran, D. P., Ed.; JAI: London, 1988; Vol. 1, pp 1–31. (b) Huisgen, R. *1,3-Dipolar Cycloaddition Chemistry*; Padwa, A., Ed.; 1984; Vol. 1, pp 1–1768.
4. (a) Silva, M. A.; Goodman, J. M. *Tetrahedron* **2002**, *56*, 3667–3671. (b) DiValentin, C.; Freccero, M.; Gandolfi, R.; Rastelli, A. *J. Org. Chem.* **2000**, *65*, 6112–6120. (c) Carda, M.; Portoles, R.; Murga, J.; Uriel, S.; Marco, J. A.; Domingo, L. R.; Zaragoza, R. J.; Roper, H. *J. Org. Chem.* **2000**, *65*, 7000–7009. (d) Liu, J.; Niwayama, S.; You, Y.; Houk, K. N. *J. Org. Chem.* **1998**, *63*, 1064–1073. (e) Annunziata, R.; Benaglia, M.; Cinquini, M.; Cozzi, F.; Raimondi, L. *Eur. J. Org. Chem.* **1998**, 1823–1832. (f) Cossio, F. P.; Morao, I.; Jiao, H.; Scheleyer, P. V. R. *J. Am. Chem. Soc.* **1999**, *121*, 6737–6746.
5. Domingo, L. R. *Eur. J. Org. Chem.* **2000**, 2265–2272.
6. Merino, P.; Anoro, S.; Merchan, F. L.; Tejero, T. *Heterocycles* **2000**, *53*, 861–875.
7. Tanaka, J.; Kanemasa, S. *Tetrahedron* **2001**, *57*, 899–905.
8. Hu, Y.; Houk, K. N. *Tetrahedron* **2000**, *56*, 8239–8243.
9. (a) Casuscelli, F.; Chiacchio, U.; Di Bella, M. R.; Rescifina, A.; Romeo, G.; Romeo, R.; Uccella, N. *Tetrahedron* **1995**, *51*, 8605–8612. (b) Chiacchio, U.; Gumina, G.; Rescifina, A.; Romeo, R.; Uccella, N.; Casuscelli, F.; Piperno, A.; Romeo, G. *Tetrahedron* **1996**, *52*, 8889–8898. (c) Chiacchio, U.; Rescifina, A.; Iannazzo, D.; Romeo, G. *J. Org. Chem.* **1999**, *64*, 28–36. (d) Chiacchio, U.; Corsaro, A.; Iannazzo, D.; Piperno, A.; Procopio, A.; Rescifina, A.; Romeo, G.; Romeo, R. *Eur. J. Org. Chem.* **2001**, 1893–1898.
10. See inter alia: (a) Bravo, P.; Bruche, L.; Fronza, G.; Zecchi, G. *Tetrahedron* **1992**, *48*, 9775–9788. (b) Tokunaga, Y.; Ihara, M.; Fukumoto, K. *Tetrahedron Lett.* **1996**, *37*, 6157–6160. (c) Ahn, C.; Kennington, J. W., Jr.; DeShong, P. *J. Org. Chem.* **1994**, *59*, 6282–6286. (d) Jensen, K. B.; Hazell, R. G.; Jorgensen, K. A. *J. Org. Chem.* **1999**, *64*, 2353–2360. (e) Conti, P.; Roda, G.; Negra, F. F. B. *Tetrahedron: Asymmetry* **2001**, *12*, 1363–1367. (f) Vasella, A.; Voeffray, R. *Helv. Chim. Acta* **1982**, *65*, 1134–1144. (g) Tamura, O.; Okabe, T.; Yamaguchi, T.; Kotani, J.; Gotanda, K.; Sakamoto, M. *Tetrahedron* **1995**, *51*, 119–128. (h) Tamura, O.; Mita, N.; Okabe, T.; Yamaguchi, Y.; Fukushima, C.; Yamashita, M.; Morita, Y.; Morita, N.; Ishibashi, H.; Sakamoto, M. *J. Org. Chem.* **2001**, *66*, 2602–2610.
11. Inouye, Y.; Watanabe, Y.; Takahashi, S.; Kakisawa, H. *Bull. Chem. Soc. Jpn* **1979**, *52*, 763–3764.
12. (a) Inouye, Y.; Hara, J.; Kakisawa, H. *Chem. Lett.* **1980**, 1407–1410. (b) DeShong, P.; Dicken, C. M.; Staib, R. R.; Freyer, A. J.; Weinreb, S. M. *J. Org. Chem.* **1982**, *47*, 4397–4403.
13. Emmons, W. D. *J. Am. Chem. Soc.* **1957**, *79*, 5739–5749.
14. Kanemasa, S.; Tsuruoka, T. *Chem. Lett.* **1995**, 49–50.
15. Gefflaut, T.; Bauer, U.; Airola, K.; Koskinen, A. M. P. *Tetrahedron: Asymmetry* **1996**, *7*, 3099–3102.
16. (a) Ito, M.; Kibayashi, C. *Tetrahedron* **1991**, *47*, 9329–9350. (b) Iida, H.; Kasahara, K.; Kibayashi, C. *J. Am. Chem. Soc.* **1986**, *108*, 4647–4648.
17. Merino, P.; Revuelta, J.; Tejero, T.; Chiacchio, U.; Rescifina, A.; Piperno, A.; Romeo, G. *Tetrahedron: Asymmetry* **2002**, *13*, 167–172.
18. Frisch, M. J.; Trucks, G. W.; Schlegel, H. B.; Scuseria, G. E.; Robb, M. A.; Cheeseman, J. R.; Zakrzewski, V. G.; Montgomery J. A., Jr.; Stratmann, R. E.; Burant, J. C.; Dapprich, S.; Millam, J. M.; Daniels, A. D.; Kudin, K. N.; Strain, M. C.; Farkas, O.; Tomasi, J.; Barone, V.; Cossi, M.; Cammi, R.; Mennucci, B.; Pomelli, C.; Adamo, C.; Clifford, S.; Ochterski, J.; Petersson, G. A.; Ayala, P. Y.; Cui, Q.; Morokuma, K.; Malick, D. K.; Rabuck, A. D.; Raghavachari, K.; Foresman, J. B.; Cioslowski, J.; Ortiz, J. V.; Stefanov, B. B.; Liu, G.; Liashenko, A.; Piskorz, P.; Komaromi, I.; Gomperts, R.; Martin, R. L.; Fox, D. J.; Keith, T.; Al-Laham, M. A.; Peng, C. Y.; Nanayakkara, A.; Gonzalez, C.; Challacombe, M.; Gill, P. M. W.; Johnson, B.; Chen, W.; Wong, M. W.; Andres, J. L.; Gonzalez, C.; Head-Gordon, M.; Replogle, E. S.; Pople, J. A. *GAUSSIAN 98 Revision A.9*; Gaussian, Inc.: Pittsburgh PA, 1999.
19. (a) Becke, A. D. *J. Chem. Phys.* **1993**, *98*, 5648–5652. (b) Becke, A. D. *Phys. Rev. A* **1988**, *38*, 3098–3100. (c) Lee, C.; Yang, W.; Parr, R. G. *Phys. Rev. B* **1988**, *37*, 785–789.
20. Reed, A. E.; Weinstock, R. B.; Weinhold, F. *J. Chem. Phys.* **1985**, *83*, 735–746.
21. Hehre, W. J.; Radom, L.; Schleyer, P. V. R.; Pople, J. A. *Ab initio Molecular Orbital Theory*; Wiley: New York, 1986.
22. (a) Fukui, K. *Acc. Chem. Res.* **1981**, *14*, 363–368. (b) Head-Gordon, M.; Pople, J. A. *J. Chem. Phys.* **1988**, *89*, 5777–5786.
23. Avalos, M.; Babiano, R.; Clemente, F. R.; Cintas, P.; Gordillo, R.; Jimenez, J. L.; Palacios, J. C. *J. Org. Chem.* **2000**, *65*, 8251–8259.
24. Aroney, M. J.; Bruce, E. A. W.; John, I. G.; Radom, L.; Ritchie, G. L. D. *Aust. J. Chem.* **1976**, *29*, 581–587.
25. Weinhold, F. *Encyclopedia of Computational Chemistry*; Schleyer, P. v. R., Allinger, N. L., Clark, T., Gasteiger, J., Kollman, P. A., Schaefer, H. F., III, Schreiner, P. R., Eds.; Wiley: Chichester, UK, 1998; Vol. 3, pp 1792–1811.
26. Mayo, P.; Hecnar, T.; Tam, W. *Tetrahedron* **2001**, *57*, 5931–5941.
27. (a) Molder, U.; Burk, P.; Koppel, I. A. *Int. J. Quant. Chem.* **2001**, *82*, 73–85. (b) Proft, F. D.; Martin, J. M. L.; Geerlings, P. *Chem. Phys. Lett.* **1996**, *250*, 393–401. (c) Geerlings, P.; Proft, F. D.; Martin, J. M. L. *Theoretical and Computational Chemistry*; Seminario, J. Ed.; Elsevier: Amsterdam, 1996; Vol. 5, p 773.
28. (a) Parr, R. G.; Pearson, R. G. *J. Am. Chem. Soc.* **1983**, *105*, 7512–7516. (b) Parr, R. G.; Yang, W. *Density Functional Theory of Atoms and Molecules*; Oxford University: New York, 1989.
29. Parr, R. G.; Donnelly, R. A.; Levy, M.; Palke, W. E. *J. Chem. Phys.* **1978**, *68*, 3801–3807.
30. (a) Pearson, R. G. *J. Chem. Ed.* **1987**, *64*, 561–567. (b) Parr, R. G.; Chattaraj, P. K. *J. Am. Chem. Soc.* **1991**, *113*, 1854–1855.
31. Parr, R. G.; von Szentpály, L.; Liu, S. *J. Am. Chem. Soc.* **1999**, *121*, 1922–1924.
32. Domingo, L. R.; Aurell, M. J.; Perez, P.; Contreras, R. *Tetrahedron* **2002**, *58*, 4417–4423.
33. Perez, P.; Domingo, L. R.; Aurell, M. J.; Contreras, R. *Tetrahedron* **2003**. We are grateful to Prof. L. R., Domingo (University of Valencia, Spain) for providing us with a copy of the manuscript in press.
34. (a) Chandra, A. K.; Nguyen, M. T. *J. Phys. Chem. A* **1998**, *102*, 6181–6185. (b) Chandra, A. K.; Nguyen, M. T. *J. Comput.*

Chem. **1998**, *19*, 195–202. (c) Nguyen, T. L.; De Proft, F.; Chandra, A. K.; Uchimaru, T.; Nguyen, M. T.; Geerlings, P. *J. Org. Chem.* **2001**, *66*, 6096–6103. (d) Sengupta, D.; Chandra, A. K.; Nguyen, M. T. *J. Org. Chem.* **1997**, *62*, 6404–6406. (e) Damoun, S.; Woude, Van de; Mendez, F.; Geerlings, P. *J. Phys. Chem. A* **1997**, *101*, 886–893.

35. Chandra, A. K.; Nguyen, M. T.; Int, *J. Mol. Sci.* **2002**, *3*, 310–323.
36. (a) Mendez, F.; Gazquez, J. L. *J. Am. Chem. Soc.* **1994**, *116*, 9298–9301. (b) Yang, W.; Mortier, W. J. *J. Am. Chem. Soc.* **1986**, *108*, 5708–5711. (c) Yang, W.; Parr, R. G. *Proc. Natl Acad. Sci. USA* **1983**, *82*, 6723.
37. (a) Loncharich, R. J.; Brown, F. K.; Houk, K. N. *J. Org. Chem.* **1989**, *54*, 1129–1134. (b) Birney, D. M.; Houk, K. N. *J. Am. Chem. Soc.* **1990**, *112*, 4127–4133. (c) Apeloig, Y.; Matzer, E. *J. Am. Chem. Soc.* **1995**, *117*, 5375–5376.
38. (a) Inouye, Y.; Watanabe, Y.; Takahashi, S.; Kakisawa, H. *Bull. Chem. Soc. Jpn* **1979**, *52*, 3763–3764. (b) Gefflaut, T.; Bauer, U.; Airola, K.; Koskinen, A. M. P. *Tetrahedron: Asymmetry* **1996**, *7*, 3099–3102. (c) Casuscelli, F.; Di Bella, M. R.; Ficarra, R.; Melardi, S.; Romeo, G.; Chiacchio, U.; Rescifina, A. *Gazz. Chim. It.* **1997**, *127*, 367–371. (d) Ondruš, V.; Orság, M.; Fišera, L'.; Prónayová, N. *Tetrahedron* **1999**, *55*, 10425–10436. (e) Tamura, O.; Yoshida, S.; Sugita, H.; Mita, N.; Uyama, Y.; Morita, N.; Ishiguro, M.; Kawasaki, T.; Ishibashi, H.; Sakamoto, M. *Synlett* **2000**, 1553–1556. (f) Kubáň, J.; Kolarovič, A.; Fišera, L.; Jäger, V.; Humpa, O.; Prónayová, N. *Synlett* **2001**, 1862–1865. (g) Chiacchio, U.; Corsaro, A.; Iannazzo, D.; Piperno, A.; Procopio, A.; Rescifina, A.; Romeo, G.; Romeo, R. *Eur. J. Org. Chem.* **2001**, 1893–1898. (h) Chiacchio, U.; Corsaro, A.; Iannazzo, D.; Piperno, A.; Rescifina, A.; Romeo, R.; Romeo, G. *Tetrahedron Lett.* **2001**, *42*, 1777–1780. (i) Chiacchio, U.; Corsaro, A.; Pistarà, V.; Rescifina, A.; Iannazzo, D.; Piperno, A.; Romeo, G.; Romeo, R.; Grassi, G. *Eur. J. Org. Chem.* **2002**, 1206–1212. (j) Merino, P.; Revuelta, J.; Tejero, T.; Chiacchio, U.; Rescifina, A.; Piperno, A.; Romeo, G. *Tetrahedron: Asymmetry* **2002**, *13*, 167–172.
39. Tietze, L. F.; Fennen, J.; Geibler, H.; Schulz, G.; Anders, E. *Liebigs Ann.* **1995**, 1681–1687.
40. Wiberg, K. B. *Tetrahedron* **1968**, *24*, 1083–1096.
41. (a) Carpenter, J. E.; Weinhold, F. *J. Mol. Struct.: Theochem* **1988**, *169*, 41–62. (b) Reed, A. E.; Weinstock, R. B.; Weinhold, F. *J. Chem. Phys.* **1985**, *83*, 735–746.
42. (a) Tokunaga, Y.; Ihara, M.; Fukumoto, K. *Tetrahedron Lett.* **1996**, *37*, 6157–6160. (b) Chiacchio, U.; Gumina, G.; Rescifina, A.; Romeo, R.; Uccella, N.; Casuscelli, F.; Piperno, A.; Romeo, G. *Tetrahedron* **1996**, *52*, 8889–8898.
43. (a) Domingo, L. R. *J. Org. Chem.* **1999**, *64*, 3922–3929. (b) Domingo, L. R.; Arnó, M.; Andrés, J. *J. Org. Chem.* **1999**, *64*, 5867–5875. (c) Domingo, L. R.; Asensio, A. *J. Org. Chem.* **2000**, *65*, 1076–1083.
44. For an example on this topic see: Liu, J.; Niwayama, S.; You, Y.; Houk, K. N. *J. Org. Chem.* **1998**, *63*, 1064–1073.